SCIENTIFIC REPORTS

OPEN

SUBJECT AREAS:
MATERIALS FOR ENERGY AND CATALYSIS
SURFACES, INTERFACES AND THIN FILMS

Received
9 September 2014

Accepted
23 October 2014

Published
11 November 2014

Correspondence and requests for materials should be addressed to L.M. (miaolei@ms.giec.ac.cn)

Solution-Processed VO_2-SiO_2 Composite Films with Simultaneously Enhanced Luminous Transmittance, Solar Modulation Ability and Anti-Oxidation property

Lili Zhao[1,2], Lei Miao[1], Chengyan Liu[1], Chao Li[1], Toru Asaka[3], Yipu Kang[3], Yuji Iwamoto[3], Sakae Tanemura[1,4], Hui Gu[5] & Huirong Su[6]

[1]Key Laboratory of Renewable Energy, Guangzhou Institute of Energy Conversion, Chinese Academy of Sciences, Guangzhou, 510640, China, [2]Graduate University of Chinese Academy of Sciences, Beijing, 100049, China, [3]Department of Frontier Materials, Graduate School of Engineering, Nagoya Institute of Technology, Gokiso-cho, Showa-ku, Nagoya, 466-8555, Japan, [4]Japan Fine Ceramic Center, 2-4-1 Mutsuno, Atsuta-ku, Nagoya, 456-8587, Japan, [5]State Key Laboratory of High Performance Ceramics and Superfine Microstructure, Shanghai Institute of Ceramics, Chinese Academy of Sciences, Shanghai, 200050, China, [6]Genuine Optronics Limited, Shanghai, 200235, China.

Recently, researchers spare no efforts to fabricate desirable vanadium dioxide (VO_2) film which provides simultaneously high luminous transmittance and outstanding solar modulation ability, yet progress towards the optimization of one aspect always comes at the expense of the other. Our research devotes to finding a reproducible economic solution-processed strategy for fabricating VO_2-SiO_2 composite films, with the aim of boosting the performance of both aspects. Compare to VO_2 film, an improvement of 18.9% (from 29.6% to 48.5%) in the luminous transmittance as well as an increase of 6.0% (from 9.7% to 15.7%) in solar modulation efficiency is achieved when the molar ratio of Si/V attains 0.8. Based on the effective medium theory, we simulate the optical spectra of the composite films and the best thermochromic property is obtained when the filling factor attains 0.5, which is consistent with the experimental results. Meanwhile, the improvement of chemical stability for the composite film against oxidation has been confirmed. Tungsten is introduced to reduce the phase transition temperature to the ambient temperature, while maintain the thermochromism required for application as smart window. Our research set forth a new avenue in promoting practical applications of VO_2-based thermochromic fenestration.

With the aim of reducing energy consumption in architectures, energy-efficient windows, especially "smart windows" based on chromogenic materials are considered to be good candidates for energy conservation and have attracted considerable concerns[1]. Vanadium dioxide (VO_2), a representative thermochromic material, can initiate an automatic reversible semiconductor-metal phase transition (SMT) from the monoclinic structure ($P2_1/c$, M1 phase: the most stable monoclinic phase in room temperature) to the tetragonal structure ($P4_2/mnm$, R phase) at *ca.* 68°C, giving rise to a dramatic modification of the optical properties from infrared (IR) transmitting to IR reflecting, and maintains the visible transparency, which is suitable for the application of energy-efficient windows[2–4]. To meet the requirement for large-scale implementation on architectural buildings, VO_2-based materials should satisfy the following criteria: the phase transition temperature (T_t) closes to the ambient temperature (≈25°C), the integrated luminous transparency (T_{lum}) ≥ 40% as well as the solar modulation ability (ΔT_{sol}) ≥ 10%[5].

Generally, doping metal ions with high valence (such as W^{6+}, Mo^{6+}, Nb^{5+}) is confirmed to be an effective way to reduce T_t to room temperature[6–8]. Among them, tungsten is proved to be the most effective dopant[9]. However, T_{lum} is inevitably limited to <40% if a relative high ΔT_{sol} is maintained, which cannot balance the requirements for T_{lum} and ΔT_{sol}[10]. Therefore, a tougher challenge is to simultaneously and substantially improve both of T_{lum} and ΔT_{sol} *via* an economic method. It is believed that the low visible transparency of VO_2 film originates from the

strong inner-band and inter-band absorptions in the short-wavelength range[11,12]. Experiments and calculations have demonstrated that some special dopants (such as F^- and Mg^{2+}) can serve to widen the band gap of VO_2 and induce a blue-shift of the absorption edge, leading to an increase of the visible transparency[13,14]. However, the improvement of T_{lum} is usually accompanied by a deteriorated switching behavior. Deposition of single/multi-layer antireflection (AR) layers with high reflective index dielectric materials (*i.e.*, SiO_2, ZrO_2, TiO_2) is a traditional strategy to enhance T_{lum}[15,16]. Nonetheless, it requires additional heating process and the presence of AR layer usually jeopardizes the near infrared (NIR) switching ability. Moreover, film thickness and microstructures markedly affect the optical properties and switching behaviors of VO_2-based films. The transmittance spectra for VO_2 films with various thicknesses illustrate that the improvement of T_{lum} is inevitably at the expense of ΔT_{sol}[17]. Zhou *et al.* have proposed a novel periodic porous structure with an unprecedented high visible light transmittance (81%). However, the switching efficiency is only *ca.* 23% at 2000 nm[18]. To our knowledge, the optical properties of VO_2 films obtained by the above approaches rarely can increase both T_{lum} and ΔT_{sol}, which otherwise tends to be undesirably low and constitutes a major obstacle for practical implementation of thermochromic fenestration.

A thrilling concept that nanocomposites materials comprising VO_2 nanoparticles and highly transparent materials is providing an intriguing interest due to the unique properties. Optical calculations have confirmed that VO_2 nanoparticles distributed in a dielectric matrix exhibit higher T_{lum} and better ΔT_{sol} than pure VO_2 films, which offers a novel perspective to achieve a favorable optical performance[19]. Inspired by this concept, some pioneering researches have devoted to fabricate VO_2-based composite particles and/or to cast them on glass or flexible substrate to obtain films with excellent thermochromic properties. Li *et al.* fabricated core-shell VO_2@TiO_2 composite nanopowders with both thermochromic and photocatalytic properties[20]. Gao *et al.* prepared flexible VO_2 nanocomposite foils based on SiO_2/VO_2 core/shell structures with an improved T_{lum} from 29.2% to 55.3%, while ΔT_{sol} exhibited a decrease from 13.6% to 7.5%[21]. Core-shell VO_2(M)@SiO_2 films on a transparent Teflon film were obtained by casting the hydrothermal synthesized composite nanoparticles to gain an increased visible transmittance from 31.72% to 35.96%, accompanied by a significant increase in ΔT_{sol} of 8.4%[22]. VO_2 nanocrystals dispersed in SiO_2 matrix are highlighted to be a new pathway to exhibit superior visible transmittance without compromising the NIR modulation ability as compared to conventional VO_2 thin film[23], offering a multitude of possibility for energy conservation.

To our knowledge, the V-O system is a complex binary system which contains a variety of compounds including V_2O_3, VO_2, V_2O_5 and so on. Moreover, the various polymorphs of VO_2, including VO_2 (R), VO_2 M1, VO_2 (B) and VO_2 (A), introduce a series of difficulties to fabricate pure VO_2 films with thermochromic properties[24]. As a result, an accurate control of annealing atmosphere is vital to the formation of pure VO_2 (M1). The majority of the fabrications of pure VO_2 (M1) usually demand on high-vacuum equipment, and it inevitably increases the fabrication cost and raises the complexity of the operation, which is unsuitable for the large-scale fabrication of VO_2-based intelligent window. Additionally, as we can see, previous studies on VO_2-based composite structure mainly focuses on a prior preparation of pure VO_2 (M1) particles followed by the formation of a composite structure due to the difficulties of direct fabrication of VO_2-based composite structure, which are closely related to the hard-controllable annealing atmosphere. Due to the above reasons, it is really significant and challengeable to develop an available pathway for directly fabricating VO_2-based composite films without the complex vacuum process, thus offering a unique opportunity to the practicable application of thermochromic coatings as "smart windows".

Differ from the composite structure usually obtained *via* a two-step process, here we present a direct synthesis of VO_2-SiO_2 composite films on glass substrate through an economic solution-based method and a relationship is drawn between the film products and the annealing conditions. With no need of a laborious vacuum processing, pure VO_2-SiO_2 composite films (M1 phase) with different molar ratios of Si/V can be easily obtained by simply varying the gas flow of nitrogen. The influence of SiO_2 on the structure, morphology as well as optical properties are detailed evaluated. We simulate the optical spectra of the composite films based on the effective medium theory and obtain a relationship between the volume filling factor (f) and ΔT_{sol}. Next, we focus on the thermochromic properties of VO_2-SiO_2 films in the function of SiO_2 contents. Our results provide a series of well-formed composite films with simultaneously enhanced T_{lum} combined with ΔT_{sol}. The obtained results are in good agreement with our calculations. The anti-oxidation property of the composite film has also been investigated. Tungsten is introduced to reduce T_t of the composite film to the vicinity of room temperature, while maintain an excellent thermochromic property. Our work hence shortens the distance of VO_2-based thermochromic films towards smart window coatings for improved building energy conservation.

Results

Optimization of annealing parameters. To obtain the pure M phase (M1) of VO_2 thin films, the appropriate annealing parameters are investigated. Fig. 1 shows the XRD patterns of films prepared at various annealing temperatures and times. As shown in Fig. 1 (a), for film annealed at 400°C, it exhibits apparent diffraction peaks which can be indexed to the pure monoclinic structure. The

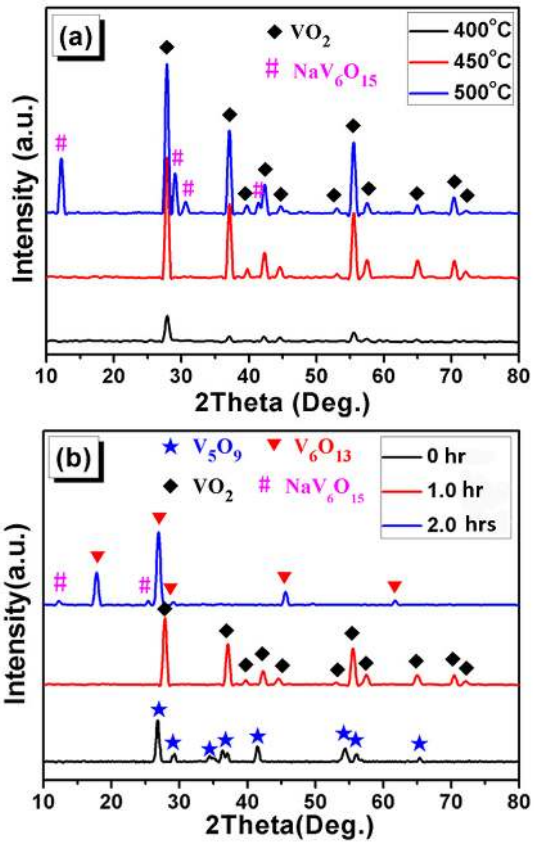

Figure 1 | XRD patterns of films prepared at different annealing conditions. (a) The annealing time is kept at 1 hour and the annealing temperature varies from 400°C to 500°C; (b) The annealing temperature is kept at 450°C and the annealing time varies from 0 hour to 2 hours.

Table 1 | The molar ratios of Si/V in the films prepared on aluminium foils and the thicknesses of the composite films on glass substrates with different Si/V molar ratios as well as the calculated filling factor according to the molar ratios of Si/V based on the EDX results. The area selected for investigation of EDX spectra is 60 × 60 μm²

Si/V molar ratio in the solution	Gas flow (L·min^{-1})	Si/V molar ratio in the films	Filling factor (f)	Film thickness (nm)
0	0.200	0	0	102
0.2	0.250	0.23	0.261	109
0.4	0.300	0.45	0.408	117
0.6	0.375	0.62	0.487	128
0.8	0.450	0.83	0.560	136
1.0	0.525	1.12	0.623	144

intensities of the diffraction peaks significantly increase as enhancing the annealing temperature to 450°C, indicating an improved crystallinity of the film. Some additional diffraction peaks which can be attributed to NaV_6O_{15} appear when the annealing temperature further increases to 500°C. The emergence of NaV_6O_{15} could be particularly originated from the diffusion of Na^+ from glass substrates as increasing the annealing temperature[25]. Fig. 1 (b) shows the XRD patterns of films annealed at 450°C for different annealing times. The nitrogen atmosphere, which contains *ca.* 0.01% O_2, greatly affects the oxidation state of the films. The main products with different annealing times are V_5O_9, VO_2 and V_6O_{13}, respectively. Additionally, NaV_6O_{15} appears when the annealing time is long. Based on the above discussion, the optimized annealing temperature and time to obtain pure M1 phase VO_2 thin film are 450°C and 1 hour, respectively.

In the above discussion for the fabrication of pristine VO_2 film, we choose the nitrogen gas as the annealing atmosphere with a gas flow of 0.200 L·min^{-1}. However, this annealing parameter suitable for pristine VO_2 film is inapplicable for VO_2-SiO_2 composite films. For example, when Si/V = 1.0, the composite film annealed under this gas flow is characterized as an amorphous carbon film with gray color. The formation of this amorphous film can be possibly attributed to the carbon residues in the films due to the incomplete degradation of the organic matter originating from the addition of SiO_2 sols. The production of carbon residues possibly results in a reduction effect on the resulting amorphous films. To consume the carbon residues, a certain amount of oxygen is required to fabricate a composite film with pure M1 phase. As we have referred, the annealing treatment is operated without a vacuum supply process. Additionally, the nitrogen gas also contains a certain amount of O_2. Consequently, in the following experimental, we can adjust the content of oxygen acted on the residual carbon substance by simply varying the gas flow of the nitrogen and the crystallization to VO_2-SiO_2 composite film (Si/V molar ratio = 1.0) occurs when the gas flow is 0.525 L·min^{-1}. As such, we discuss the appropriate atmosphere for other composite films and the detailed gas flow of nitrogen for each film is listed in Table 1.

Film structure. Fig. 2 depicts the typical XRD patterns of VO_2-SiO_2 composite films with different Si/V molar ratios, which can be used to further evaluate the evolution of the phase composition, grain size, and crystallinity of the films. It is revealed that all films exhibit the typical diffraction peaks of M1 phase VO_2 (JCPDS card no. 72-0514, $P2_1/c$, a = 0.5743 nm, b = 0.4517 nm, c = 0.5375 nm, and β = 122.61°). Since the annealing temperature is far below the crystallization point of SiO_2, it is most likely that the SiO_2 in the composite films is amorphous, which cannot be detected by XRD. Additionally, no evidence can be seen for other crystalline phases, such as V_2O_5, V_2O_3 or VSi_x, indicating the purity of the composite films. None of the diffraction peaks exhibit significant migration with increasing the molar ratio of Si/V. However, a broadening and weakening tendency of the diffraction peak of (011) crystalline plane is observed, which is largely due to the grain refinement as increasing the molar ratio of Si/V.

Film morphology. The morphology of the prepared films is of paramount importance to obtain the desired optical properties, and the changes in the particles size and morphology of the films induced by the addition of SiO_2 can be observed *via* SEM images. Fig. 3 exhibits the morphology evolution of the composite films upon enhancing the Si/V molar ratio. For pristine VO_2 film, the film is composed with uniform and well-formed grains. Clear grain boundaries appear between the particles. Upon the addition of SiO_2, the particle sizes are apparently depressed in Fig. 3 (b), (c) and (d), which is consistent with the earlier report[22]. The size reduction can also be confirmed in the cross-sectional SEM observation of the VO_2 film and VO_2-SiO_2 composite film (Si/V = 0.8), as illustrated in Fig. 3 (e) and (f). Compared to the pristine VO_2, the VO_2-SiO_2 composite film shows relative homogenous and narrow particle size distributions, indicating that the SiO_2 in the composite film play a crucial role to reduce the degree of growth and agglomeration of VO_2 particles. According to these observations, it may be concluded that SiO_2 particles are well formed and a composite structure is obtained in the film. With the aim to determine the effective molar ratios of Si/V in the composite films, we fabricate the films on the aluminum foils (to exclude the influence of the Si in the glass substrate) under the same procedure discussed above and the followed EDX analysis results are demonstrated in Table 1. The atomic percent ratios of Si/V are respectively *ca.* 0, 0.23, 0.45, 0.62, 0.83, 1.12, which are in close proximity to the initial ratios in the deposition solutions.

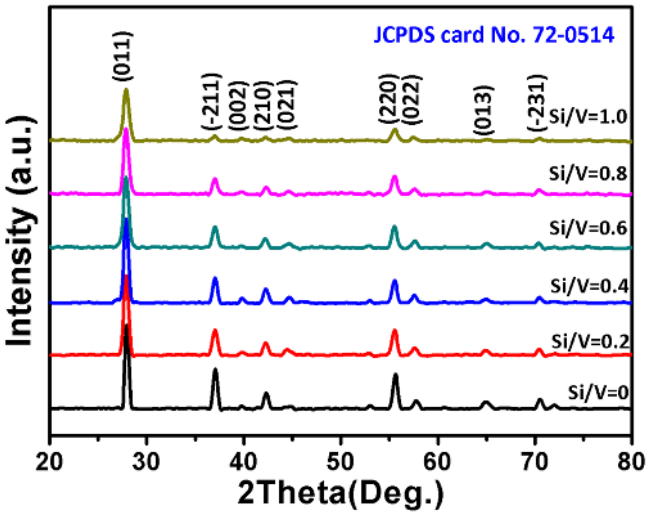

Figure 2 | XRD patterns of VO_2-SiO_2 composite films upon increasing the Si/V molar ratios in the deposition solution. The annealing temperature and time were kept at 450°C and 1 hour, respectively.

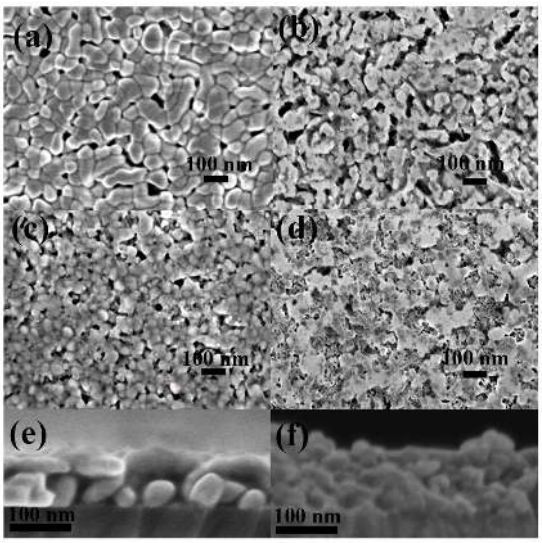

Figure 3 | The surface morphology of films with various Si/V molar ratios. Si/V = (a) 0; (b) 0.4; (c) 0.6; (d) 0.8. The cross sectional of pristine VO_2 film (e) and VO_2-SiO_2 composite film with Si/V = 0.8 (f).

To further detect the microstructure of the composite film, high-resolution transmission electron microscopy (HRTEM) images and corresponding selected area electron diffraction (SAED) patterns are collected for the VO_2-SiO_2 composite film (Si/V molar ratio = 0.8). As shown in Fig. 4 (a), the film is composed of well-fined particles, which is in agreement with the SEM images observed previously. The crystallized VO_2 and the amorphous SiO_2 particles are distributed as separate phases as shown in Fig. 4 (b). A more detailed microstructural analysis further confirms that the sample is crystallized into monoclinic VO_2. As is found in the SAED patterns (Fig. 4 (d)), bright diffraction rings evident the polycrystallinity nature of the sample, which is consistent with the XRD results. In Fig. 4 (c), clear and ordered lattice fringes are observed in the HRTEM images, corresponding to the (011) crystalline plane. The distributions of VO_2 and SiO_2 are examined by scanning transmission electron microscopy (STEM) and elemental mapping measurements. The annular dark-field (ADF) image of VO_2-SiO_2 (Fig. 4 (e), (f)) and the elemental maps respectively corresponding to V, Si and O (Fig. 4 (g), (h), (i)) further illustrate the inhomogeneous distribution of VO_2 and SiO_2 nanoparticles in the composite film. The particle sizes of VO_2 range from 30 to 100 nm, which is in good agreement with the SEM images.

Optical properties. Fig. 5 depicts the variation of visible transmittance of VO_2-SiO_2 composite films in response to the variation of Si/V molar ratios. It is clearly that the maximum visible transparency greatly enhances from 41.9% to 64.7% at 630 nm as increasing the proportion of SiO_2 in the film. Compare the insert images which represent the photographs of VO_2 and VO_2-SiO_2 films (Si/V molar ratio = 0.8), a significant enhancement of the visible transparency is observed. Lopez *et al.* have previously revealed that the scattering effect of VO_2 gradually decreases with the reduction of the particle size, indicating that the transmittance would reasonably increase[26]. The addition of SiO_2 restricts the growth and aggregation of VO_2 particles, and further reduces the initial reflectance of particles and thus inherits a better high luminous optical property, which is in consistent with the previous report[23]. In addition, the visible transmittance is enhanced possibly through an AR effect[27]. Upon the addition of SiO_2 in the composite films, SiO_2 stack on the surface of VO_2 particles and serve as the AR layer, which can effectively affect the reflected light from the air-coating and coating-substrate interfaces, leading to a higher transmittance over the visible region spectrum[28]. Wavelength dependent refractive indices (n) and extinction coefficient (k) of VO_2-SiO_2 composite films with various Si/V molar ratios are plotted in Fig. 6. Expectedly, both the n and k of the composite thin films exhibit a significant depression in whole measured wavelength upon the increase of SiO_2 addition. Fig. 7 illustrates the reflectance spectra of VO_2-SiO_2 composite films of the semiconductor state. Upon the addition of SiO_2 in the composite film, the reflectance shows a significant depression in the whole wavelength. According to the Fresnel's equation[29], the reduced n (2.58 for VO_2 film and 2.30 for

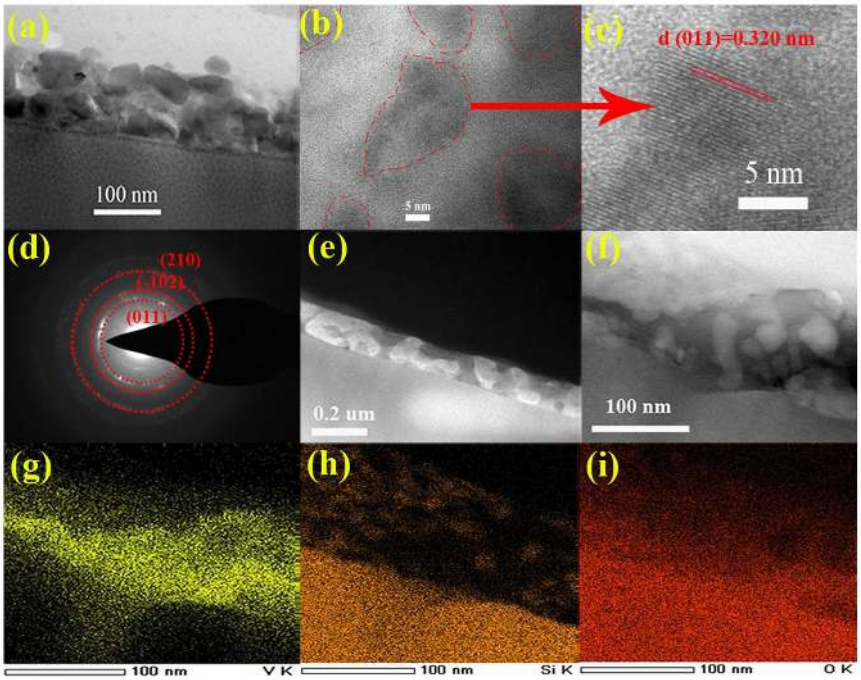

Figure 4 | The TEM image (a), HRTEM (b, c), SAED patterns (d), ADF (e, f) images of the VO_2-SiO_2 composite film (Si/V = 0.8) and the elemental maps respectively corresponding to V, Si and O ((g), (h), (i)).

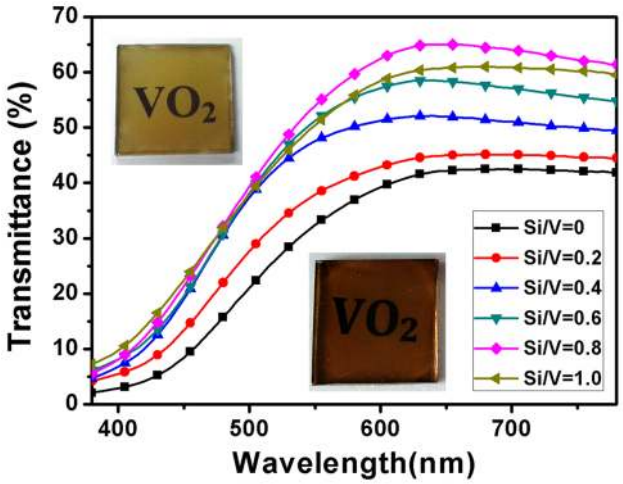

Figure 5 | The luminous transmittance of films with different Si/V molar ratios ranges from 380–780 nm measured at 30°C. The insert images correspond respectively to photographs of the pristine VO_2 film (below) and VO_2-SiO_2 composite film (Si/V = 0.8) (upper).

VO_2-SiO_2 film with Si/V = 1.0) contributes to a decreased reflectance of the film.

The spectral transmittance of VO_2-SiO_2 composite films of the semiconductor state ranges from 250 nm to 2500 nm are characterized as shown in Fig. 8. VO_2 thin film exhibits salient switching of the NIR transmittance, indicating a good thermochromic property. Especially, the composite films show better optical performance with a larger transmittance change in 2000 nm (ΔT_{200nm}) upon the

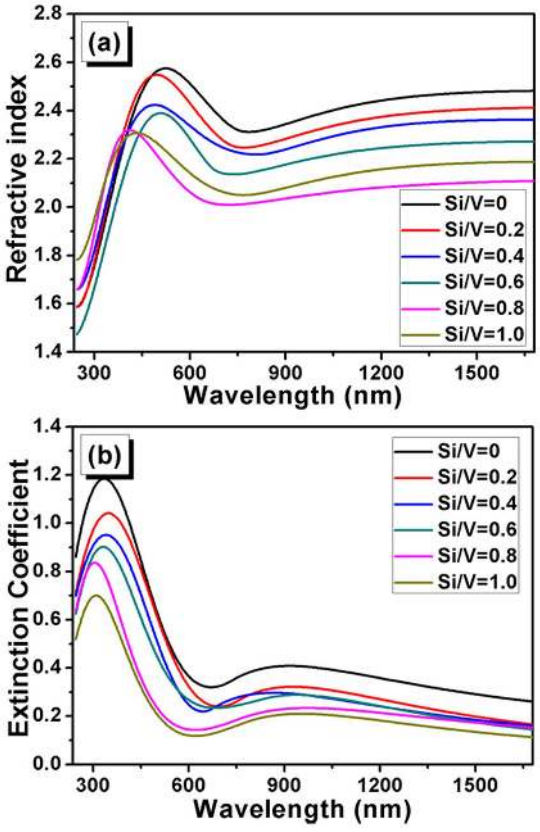

Figure 6 | The wavelength dependent refractive index (a) and extinction coefficient (b) of films with different Si/V molar ratios. All of the optical constants are measured at 30°C.

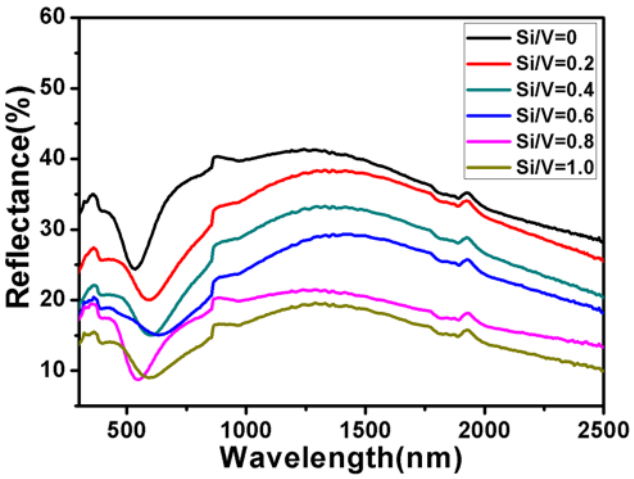

Figure 7 | The reflectance spectra measured at 30°C of VO_2-SiO_2 composite films with different Si/V molar ratios range from 250 to 2500 nm.

increase in the addition of SiO_2, as shown in Table 2. The phenomenon is consistent with the previously studies that not only the luminous transmittance but also the transmittance change upon the phase transition greatly increase with the decrease of VO_2 particle size[30]. To further quantify the potential application of the composite films as coatings on smart windows, we calculate the integral luminous transmittance (T_{lum}, 380–780 nm) and solar transmittance (T_{sol}, 250–2500 nm) of all the composite films based on the measured spectra using the following expression:

$$T_{lum/sol} = \frac{\int \varphi_{lum/sol}(\lambda)T(\lambda)d\lambda}{\int \varphi_{lum/sol}(\lambda)d\lambda} \quad (1)$$

where $T(\lambda)$denotes the transmittance at wavelength λ, φ_{lum} is the standard luminous efficiency function for the photopic vision of human eyes and φ_{sol} is the solar spectral irradiance for the air mass 1.5 (The receiving surface is defined as an inclined plane at 37° tilt toward the equator)[31]. The luminous transmittance modulation (ΔT_{lum}) and solar energy modulation (ΔT_{sol}) are defined as:

$$\Delta T_{lum} = T_{lum,s} - T_{lum,m} \quad (2)$$

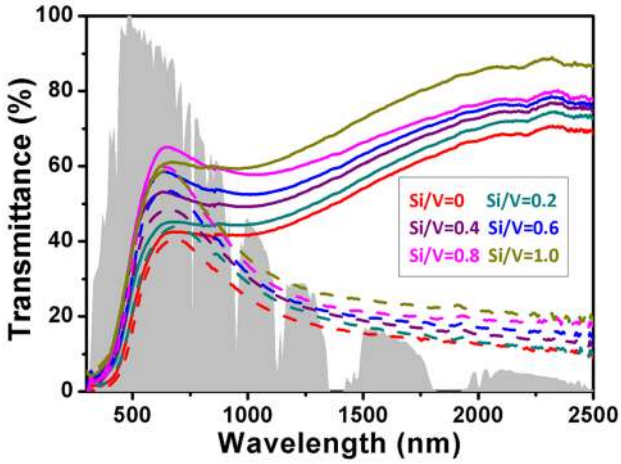

Figure 8 | Transmittance spectra of VO_2-SiO_2 composite films upon increasing Si/V molar ratios in the wavelength ranges from 250 nm to 2500 nm. Solid line: 30°C; Dash line: 100°C. The gray area indicates the normalized values of the solar spectral irradiance (φ_{sol}).

Table 2 | Optical parameters during the phase transition of VO_2-SiO_2 films with different Si/V molar ratios

Si/V molar ratio	T_{550nm}	$\Delta T_{2000\ nm}$	$T_{lum,s}$	$T_{lum,m}$	ΔT_{lum}	$T_{sol,s}$	$T_{sol,m}$	ΔT_{sol}
0	32.5	54.2	29.6	26.8	2.8	35.2	25.5	9.7
0.2	37.9	56.8	33.7	30.4	3.3	39.7	27.8	11.9
0.4	47.5	56.7	40.7	36.3	4.4	44.9	31.8	13.1
0.6	51.3	57.7	44.5	39.5	5.0	48.8	34.0	14.8
0.8	53.9	57.4	48.5	43.2	5.3	52.9	37.2	15.7
1.0	50.5	60.7	46.4	42.5	3.9	54.2	38.8	15.4

$$\Delta T_{sol} = T_{sol,s} - T_{sol,m} \quad (3)$$

$T_{lum,s}$, $T_{lum,m}$, $T_{sol,s}$ and $T_{sol,m}$ denote as the luminous transmittance and solar transmittance at the semiconducting state and the metallic state, respectively. The obtained results are elaborated in Table 2. It is clear that the ΔT_{sol} greatly increases from 9.7% for VO_2 thin film to a maximum of 15.7% when Si/V molar ratio attains 0.8, accompanied by a huge increment of $T_{lum,s}$ from 29.6% to 48.5%. The obtained values are the best among the reported values of T_{lum} and ΔT_{sol} for a typical single-layered VO_2 film (41.0%, 6.7%)[27], TiO_2/VO_2 double-layered films (46.0%, 7.0%)[32], $TiO_2/VO_2/TiO_2/VO_2/TiO_2$ five-layered films (44%, 12.1%)[33], VO_2-Sb:SnO_2 composite films (49.8%, 11.7%)[34] and core-shell VO_2(M)@SiO_2 casted foils (35.9%, 8.4%)[22].

Phase transition temperature. The switching characteristics of the composite films are investigated by recording the temperature-dependent optical transmittance during the heating and cooling process at 2000 nm as illustrated in Fig. 9. Detailed parameters of the hysteresis loops are obtained as follows. Briefly, a plot of $d(Tr)/d(T)$ &T is obtained from each hysteresis loop, yielding two peaks with a well-defined maximum. Tr and T denote as the transmittance and temperature, respectively. Each $d(Tr)/d(T)$ &T curve has been fitted with a Gaussian function using the Origin pro 8.0 software, as shown in Fig. 10. The temperature corresponding to the maximum of each $d(Tr)/d(T)$&T curve is defined as the phase transition temperature of heating and cooling branch, denote as T_h and T_c, respectively. The phase transition temperature (T_t) of the film is defined as:

$$T_t = (T_h + T_c)/2 \quad (4)$$

The hysteresis loop width (ΔT_t) is defined as the difference between T_h and T_c. The sharpness of the phase transition for heating or cooling run is characterized by the full width at half maximum ($FWHM$) of the $d(Tr)/d(T)$ &T curve, smaller value means sharper change of the slope. The detailed parameters are summarized in Table 3.

As we can see, a large hysteresis of the pristine VO_2 thin film, of around 9.9°C, is directly related to the nanoparticle microstructure[31]. Broader hysteresis loops are obtained for samples with the addition of SiO_2. It is striking to notice that by continuously increasing the Si/V molar ratios, T_c of the film shows no obvious variation, while T_h exhibits a progressive increase. Meanwhile, the transition sharpness becomes smoother (expressed as the apparent enhancement of $FWHM$) upon enhancing the Si/V molar ratio. We ascribe this phenomenon to the surrounding SiO_2, which helps to absorb the locally induced stresses among VO_2 lattices during the phase transition[23].

Anti-oxidation properties. The poor long-term oxidation resistance is another obstacle to the application of smart windows due to the thermodynamically instability of VO_2. It has been previously reported that VO_2 is gradually oxidized into toxic V_2O_5 when it is exposed to the air for a long period or abused at high temperature above 300°C[35–37], which leads to a considerable deterioration of the thermochromic properties. In this case, improving the chemical stability of VO_2 against oxidation is urgently required. The anti-oxidation properties of the film after the addition of inert SiO_2 are investigated compared with the pristine VO_2 thin film. As illustrated in Fig. 11, after expositing the films in air at room temperature for 6 months, the pristine VO_2 film cannot maintain the original pure monoclinic phase with the (011) peak weakens while some additional peaks assigned to V_2O_5 appear. For the composite film (Si/V molar ratio = 0.8), the XRD pattern shows no obvious change and all peaks can be assigned to the monoclinic VO_2. The results firmly confirmed that the addition of SiO_2 in the composite structure can effectively protect VO_2 from being oxidized, offering a similar anti-oxidation protection comparable to the anti-reflection layer[27].

Tungsten doped VO_2-SiO_2 composite film. For our VO_2-SiO_2 composite film, the simultaneously enhanced luminous transparency and the solar energy modulation have met the requirements ($T_{lum} \geq 40\%$, $\Delta T_{sol} \geq 10\%$). Although, the T_t of the composite film increase upon the addition of SiO_2, it can be readily reduced to the ambient temperature by replacing some vanadium atoms with tungsten. Fig. 12 shows the XRD pattern, transmittance spectra as well as the hysteresis loop of W-doped

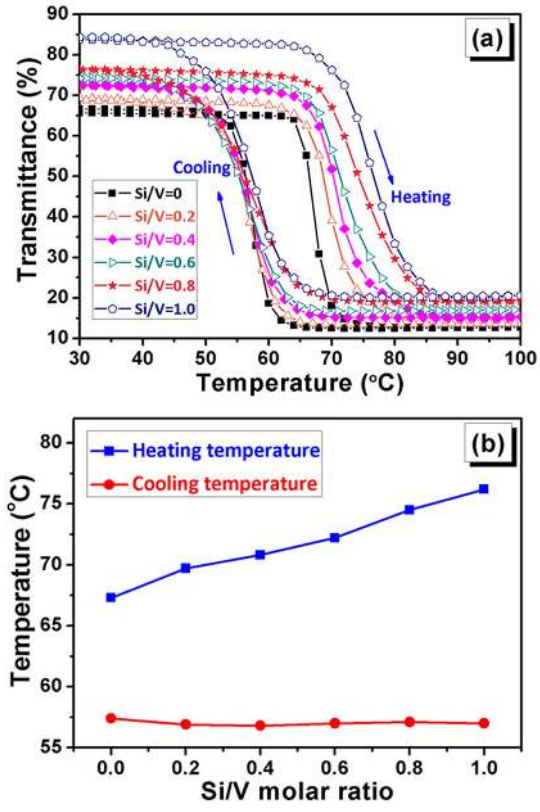

Figure 9 | (a) The hysteresis loops at 2000 nm of VO_2-SiO_2 composite films with different Si/V molar ratios. (b) The relationship between the transition temperature and the Si/V molar ratio during the heating and cooling processes.

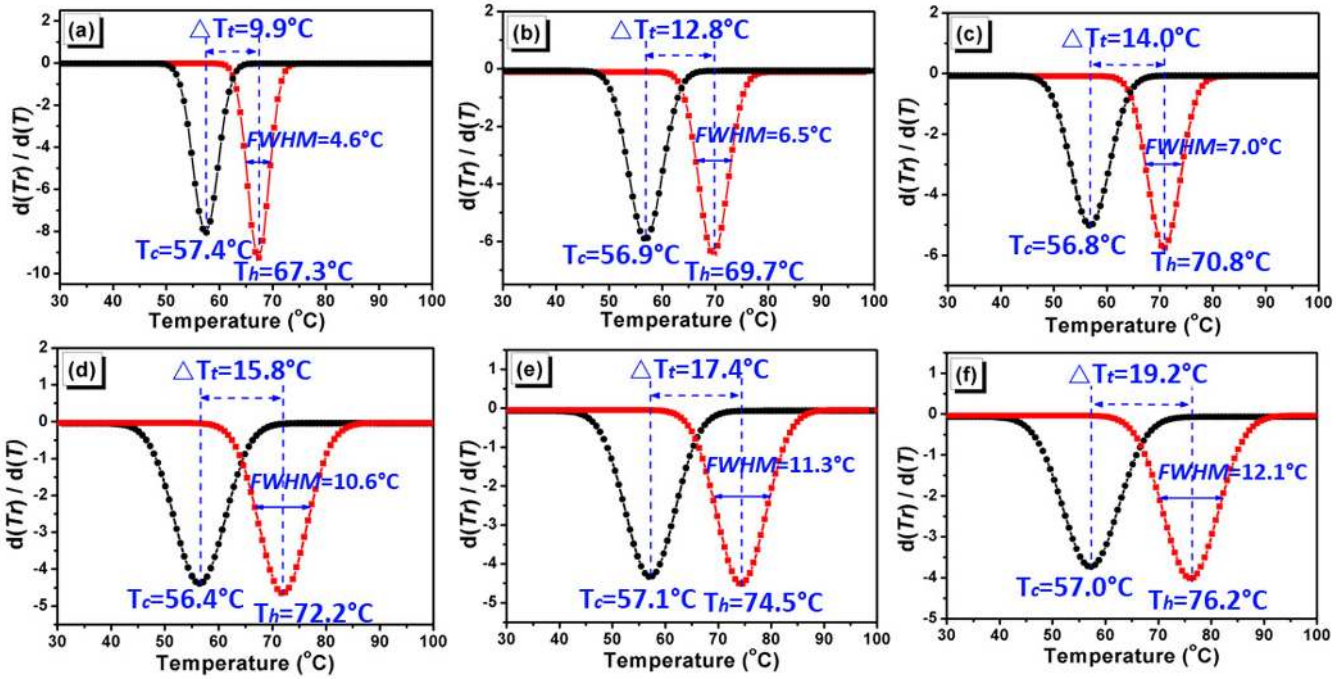

Figure 10 | The $d(Tr)/d(T)$&T plots of VO_2-SiO_2 composite films with different Si/V molar ratios to describe the transition parameters of heating and cooling branches. The molar ratio of Si/V = (a) 0; (b) 0.2; (c) 0.4; (d) 0.6; (e) 0.8; (f) 1.0. Tr and T represent transmittance and temperature at 2000 nm. T_h and T_c express the phase transition temperature of heating and cooling branches, respectively.

VO_2-SiO_2 composite film (molar ratio: W/V = 0.015; Si/V = 0.8). The composite film exhibits pure monoclinic structure as well as significant transmittance change in NIR spectrum across the phase transition. The phase transition temperature is successfully reduced to 34.2°C and the hysteresis loop width is also narrowed down by 3.8°C. The NIR switching efficiency is diminished compared with undoped film due to the incorporation of W dopant. Nonetheless, T_{lum} and ΔT_{sol} of the W-doped composite film are calculated to be respectively 43.3% and 11.3%, satisfying the requirements for practical thermochromic fenestration.

Discussion

In order to give a deeper analysis for the change of optical properties upon the addition of SiO_2, we simulate the optical spectra of the composite films as shown in Fig. 13. Clear evidence for thermochromism is seen in reflectance (R) and transmittance (T) regardless of the volume filling factor (f). The R (T) of the semiconductor state exhibits a significant decrease (increase) with enhancing the f, and vice versa. T_{lum}, T_{sol}, ΔT_{sol} as well as the ΔT_{lum} of the films corresponding to each f are calculated and plotted as shown in Fig. 14. Both T_{lum} and T_{sol} demonstrate a progressive increase when f is enhanced. Meantime, not only the T_{sol} but also the T_{lum} of the semiconductor state is higher than that of the metallic state, indicating that the thermochromism is not confined to the NIR region but takes place in the whole wavelength. Moreover, it can be referred from Fig. 14 (c) that ΔT_{sol} exhibits a broad maximum of 16.07% when $f = 0.5$ and is compatible with $T_{lum,s} = 57.85\%$ and $T_{lum,m} = 51.22\%$. The calculation for VO_2 particles dispersed in In_2O_3: Sn performed by Li *et al.* exhibits a same tendency and ΔT_{sol} displays a broad maximum of *ca.* 12.8% for $f = 0.35$, which is close to the value where the VO_2 units start to percolate in the Bruggeman model[38].

As we have noted, the ΔT_{sol} greatly increases from 9.7% for VO_2 thin film to a maximum of 15.7% when Si/V molar ratio attains 0.8 (corresponds to $f = 0.56$), accompanied by a huge increment of $T_{lum,s}$ from 29.6% to 48.5%. The experimental results are in good agreement with the calculations. The synergistic performances suggest that high T_{lum} and excellent ΔT_{sol} can be realized simultaneously *via* optimizing the f of SiO_2 in the composite film, which paves a new way for the application of VO_2-based smart windows.

Table 3 | The detail parameters derived from the hysteresis loops at 2000 nm of VO_2-SiO_2 composite films with different Si/V molar ratios

Si/V molar ratio	T_h(°C)	T_c(°C)	T_t(°C)	ΔT_t(°C)	$FWHM$(°C)
0	67.3	57.4	62.3	9.9	4.6
0.2	69.7	56.9	63.3	12.8	6.5
0.4	70.8	56.8	63.8	14.0	7.0
0.6	72.2	56.4	64.3	15.8	10.6
0.8	74.5	57.1	65.8	17.4	11.3
1.0	76.2	57.0	66.6	19.2	12.1

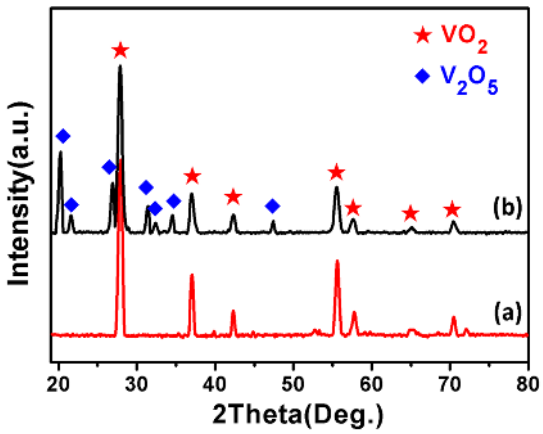

Figure 11 | The XRD patterns of pristine VO_2 film and VO_2-SiO_2 composite film (Si/V molar ratio = 0.8) after depositing in air for 6 months. (a) VO_2 film; (b) VO_2-SiO_2 composite film (Si/V molar ratio = 0.8).

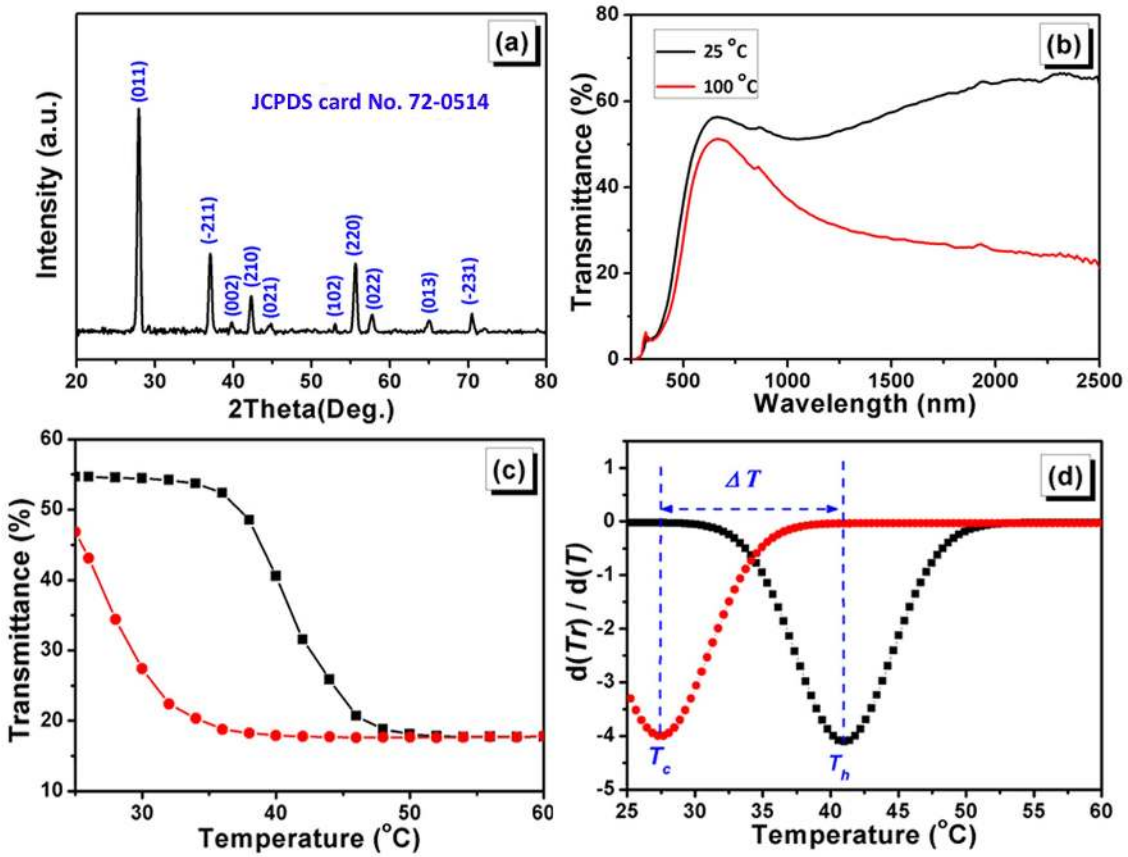

Figure 12 | JCPDS card No. 72-0514 (a), transmittance spectra at 25°C and 100°C (b), hysteresis loop at 2000 nm (c) as well as corresponding *d*(*Tr*)/*d*(*T*) &*T* plot of W-doped VO_2-SiO_2 composite film (molar ratio: W/V = 0.015; Si/V = 0.8). *Tr* and *T* represent transmittance and temperature at 2000 nm, respectively.

Our calculations mentioned above have confirmed that the thermochromism of VO_2 occurs in the entire solar range. As a result, ΔT_{sol} can be described as:

$$\Delta T_{sol} = \Delta T_{lum} + \Delta T_{nir}. \quad (5)$$

ΔT_{lum} and ΔT_{nir} denote as the integral transmittance modulation of the visible and NIR spectra, respectively. It is worthy noted that solar energy between 250–2500 nm constitutes the majorities of the total heat energy in the whole solar irradiance spectra, among which, the heat energy in the visible light and NIR light accounts for *ca.* 43% and 48%, respectively[39]. Expectedly, not only the transmittance change in the NIR region but also the changes in visible light region of VO_2 thin film to undergo the phase transition play an important role in determining the ΔT_{sol}. Previous researches have demonstrated that the change in the luminous transmittance (ΔT_{lum}, the difference between $T_{lum,s}$ and $T_{lum,m}$) of the film is thickness-dependent[40]. For film with less than 50 nm thick, $T_{lum,s}$ of the film is generally lower than $T_{lum,m}$ due to the interference effect, and, vice versa[17]. In our experiment, the thicknesses of obtained films are determined to be approximately 102, 109, 117, 128, 136 and 144 nm respectively by the step profiler (listed in Table 1), increases with the enhancement of the molar ratio of Si/V (Higher viscosity of the precursor solution is obtained when increasing the proportion of SiO_2 sols, contributing to a slight increase in film thickness due to the same spin-coating parameters.). The ΔT_{lum} value of the composite films increases as enhancing the molar ratio of Si/V (from 2.8% for Si/V = 0 to 5.3% for Si/V = 0.8), which is in line with the calculated results. Of note, with enhancing the molar ratio of Si/V in the film, the value of $\Delta T_{2000\ nm}$ for the composite film exhibits an obvious improvement compared to the VO_2 film, which, to a large extent, determines the ΔT_{nir}, giving rise to the increase of ΔT_{sol}. The improvement of ΔT_{lum}, together with the enhancement of ΔT_{nir}, jointly contribute to the larger ΔT_{sol} for films with larger Si/V molar ratio.

For our VO_2-SiO_2 composite film, T_h shows a progressive increase by continuously increasing the Si/V molar ratios, while leaving T_c unchanged. A similar phenomenon has also been observed in VO_2/Pt multi-layers due to the replacement of VO_2/air interfaces with VO_2/Pt interfaces by Pt deposition, which confirms that the VO_2 interact with the surrounding media play a role in modifying the SMT path[41,42]. To our knowledge, the occurrence of the two transitions is dominated by totally different defects. For the transition from semiconductor phase to metal phase, the vast majority of the newly formed metal-phase VO_2 nuclei are located extremely close to grain boundaries due to the surface-localized defects. While for the reversal transition, it is dominated by bulk defects in VO_2 particles[43]. The shift of T_h towards higher temperatures indicates that the SMT is retarded by nucleation of the metal phase after the change of surrounding medium. The diminished availability of defects which can serve as nucleation sites lowers the possibility to trigger the phase transition, contributing to the shift of T_h towards higher temperatures[44]. Furthermore, the composite films are annealed in a relative oxygen-rich atmosphere, the excess oxygen can act as an acceptor and stabilize the semiconductor state, leading to a higher T_h[45]. However, the influences of these defects on the reversal transition are much less effectively[46]. As such, the broadening of the hysteresis loops can also be ascribed to it[47]. The shift of T_h towards higher temperature gives a clue that the chemical stabilization of the semiconductor state is enhanced.

Our research provides a simple and economic solution-based method to fabricate VO_2-SiO_2 composite films with the aim to simultaneously improve the luminous transmittance and the solar energy modulation. Differ from the common method to fabricate pure VO_2

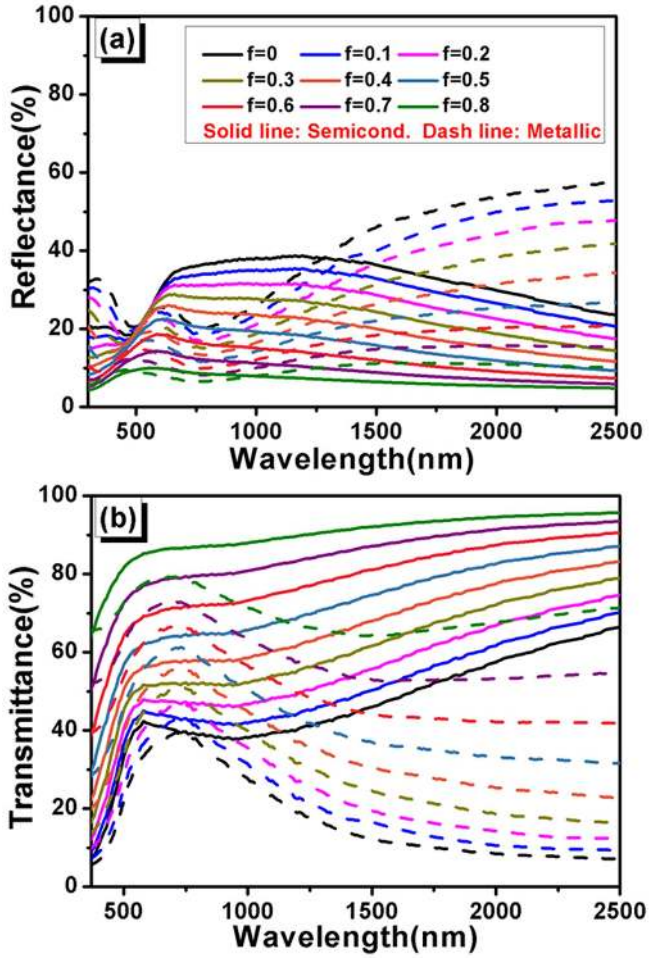

Figure 13 | The computed reflectance (a) and transmittance (b) spectra of VO_2-SiO_2 composite film with different SiO_2 volume fractions. The volume fraction of SiO_2 is denoted as *f*. Solid line: semiconducting state; Dash line: metallic state.

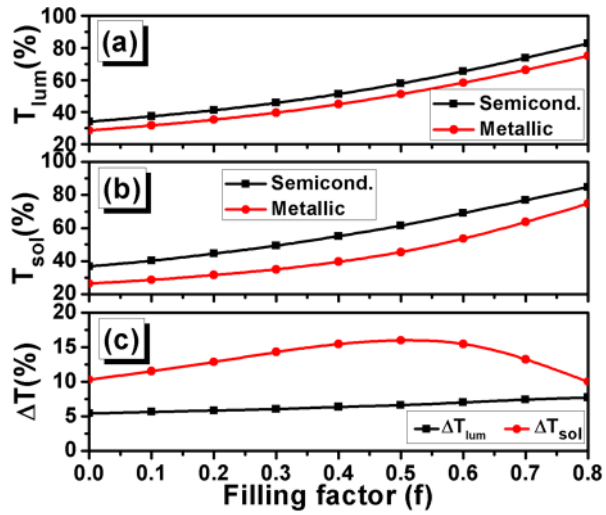

Figure 14 | Wavelength-integrated luminous (a), solar (b) transmittance, and thermochromic modulation of both the luminous transmittance and solar energy (c) based on the computed transmittance spectra as a function of *f* for VO_2-SiO_2 composite film. T_{lum}, T_{sol}, ΔT_{lum} and ΔT_{sol} refer to the integral luminous transmittance, solar transmittance, luminous transmittance modulation and solar modulation ability, respectively.

(M1), we provide an easy-controllable method by simply varying the gas flow of nitrogen and have no requirement of high-vacuum equipment. All of the obtained composite films exhibit pure monoclinic phase structure with excellent crystallinity. According to the TEM results, VO_2 and SiO_2 are distributed as separate phases and the addition of SiO_2 in the films plays an important role in hindering the growth and aggregation of VO_2.

Based on the effective medium theory, we calculate the optical constants and simulate the corresponding optical spectra of the composite films of various filling factors. The calculations illustrate that the composite film exhibits the best thermochromic property when the filling factor attains 0.5, which is consistent with the experimental result. With the exception of the high luminous transmittance and the superior modulation of solar modulation (T_{lum} = 48.5%, ΔT_{sol} = 15.7%), the anti-oxidation property of the composite film is discussed. VO_2-SiO_2 composite film maintains the original monoclinic structure after depositing in air for six months. Tungsten is introduced to effectively reduce the phase transition temperature to the ambient temperature, while retains the thermochromism required for application as smart window. Our VO_2-SiO_2 composite films enable effective tailoring of the optical performance, which open a new horizon of multifunctional coating as the architectural fenestration.

Methods

Materials. All the chemicals of analytical grade were commercially available and used without further purification. Vanadium pentoxide (V_2O_5) was chosen as the source of vanadium and oxalic acid ($H_2C_2O_4{\cdot}2H_2O$) was selected as the reducing agent. Tetraethyloxysilane (TEOS) and hydrochloric acid (HCl, 37%) were used as the silica precursor and hydrolyzing catalyst, respectively. Pluronic F127 (EO_{100}-PO_{65}-EO_{100}, M_w = 12,600 g/mol) was added as a pore-forming agent. Dehydrates ethanol (EtOH, 95%) was used as solvent in both systems. Ammonium tungstate hydrate ($(NH_4)_5H_5[H_2(WO_4)_6]{\cdot}H_2O$) was chosen as dopant to lower the phase transition temperature.

Synthesis of VO_2-SiO_2 composite thin films. The preparation process of the VO_2-SiO_2 composite films is shown schematically in Fig. 15. In a typical synthesis, certain amount of V_2O_5 was reduced by $H_2C_2O_4$ (molar ratio is 1 : 3) in EtOH solution. After refluxing at 120°C for 10 hours (hrs), a transparent blue solution of $VOC_2O_4{\cdot}xH_2O$ (1.0 M) was obtained. For preparing a VO_2-SiO_2 composite solution, a SiO_2 sol was prepared by mixing TEOS, EtOH and H_2O (The pH value was adjusted to 2 with HCl) at a given volume ratio as =1 : 10 : 0.2. F127 was added as a pore-forming agent to increase the porosity of the film. The solution was stirred for 1 hour followed by aging for at least one day before merging with the $VOC_2O_4{\cdot}xH_2O$ solution. After blending thoroughly for 1 hour, a homogeneous, clear and blue solution was obtained. The final concentration of $VOC_2O_4{\cdot}xH_2O$ was diluted to a constant of 0.5 M by EtOH and the nominal Si/V atomic ratio varied from 0 to 1.0. For tungsten doped sample, the amount of the additive was carefully controlled for the realization of a fixed W doping level up to 1.5 at.%. The precursor solutions were aged for 2 hrs at room temperature before spin coating.

Composite films were deposited on borosilicate glasses (20 × 20 mm^2) by a spin-coating technology with the speed of 3000 rpm for 20 s. To analyze the elemental composition and the molar ratio of Si/V in the composited films, films were prepared on aluminum foils under the same procedure. All the substrates were sequentially cleaned by acetone, ethanol and deionized water to remove surface contaminations. After drying at 60°C for 10 min to remove the excess solvent, the as-prepared films were annealed by the step of 5°C/min in tube furnace under an appropriate atmosphere.

Characterization. The crystal structure of the VO_2-SiO_2 composite films was collected by Glancing Angle X-ray diffractometer (GAXRD, PANalytical X'pert Pro MPD) using Cu-Kα radiation (λ = 1.54 Å). The operating voltage and current were kept at 40 kV and 40 mA, respectively. The surface morphology and element distributions were characterized by field emission scanning electron microscopy (FESEM, S-4800, Hitachi Japan) and transmission electron microscopy (TEM, 2010F, JEOL and TF20, FEI) equipped with an energy-dispersive spectrometer (EDS, Oxford) attachment. The thicknesses of the composite films were determined by the step profiler (Alpha-Step D-100, KLA-Tencor USA). Specimens for TEM analysis were prepared by cutting, grinding, dimpling and ion-milling (Gatan 691, operated at 3.0 to 0.5 kV and cooled with liquid nitrogen), followed by surface cleaning using an ion cleaner (JIC-410, JEOL Japan) to remove completely any residual amorphous film. The thermochromic properties of the films were monitored by ultraviolet-visible-near infrared spectrophotometer (UV-Vis-NIR, Lambda 750), from 250 to 2500 nm at temperature 30°C and 100°C, respectively. Temperature was measured with the assistance of a temperature sensor in contact with the films which was connected with a temperature controlling unit (FP23, SHIMADEN Japan). The

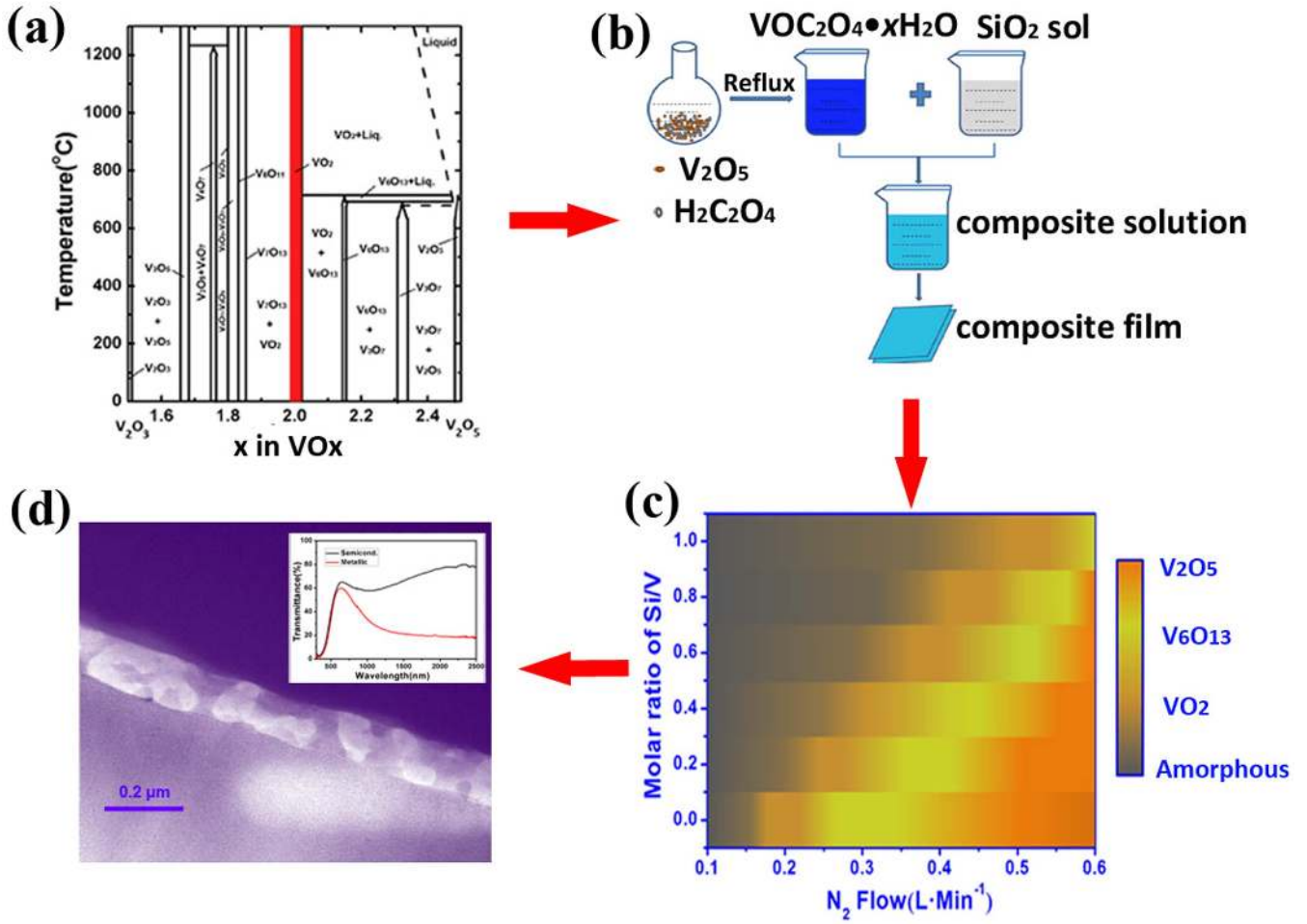

Figure 15 | (a) The phase diagrams of V-O system[52]; (b) The flow chart of the preparation procedure of the VO_2-SiO_2 composite films; (c) A relationship drawn between the annealing products and the gas flow of N_2; (d) The TEM image of the VO_2-SiO_2 composite film (Si/V molar ratio = 0.8) and the insert image is the corresponding spectrum of this sample.

refractive index and extinction coefficient of the films were performed on spectroscopic ellipsometry (SE) (M-2000UI, J.A. Woollam USA) in the spectral range of 245–1680 nm. Hysteresis loops were measured by collecting the transmittance of the films at a fixed wavelength (2000 nm) under variable temperatures at an approximate interval of 2°C. The temperature errors were less than ±1.0°C based on repeated measurements.

Calculation based on the effective medium theory. Based on the effective medium theory, we calculate the optical constants of the composite films. It is considered that there is a random mixture of VO_2 and SiO_2 nanoparticles dispersed in our composite films. Both of the nanoparticles are taken to be spherical with size far less than λ, so that the composite film can be regarded as an "effective medium" model with properties intermediate between those nanoparticles. Assuming that the VO_2 and SiO_2 units are topologically equivalent, it is appropriate to get the effective dielectric function (ε) based on the Bruggeman theory[4,48–50].

$$f\frac{\varepsilon_{SiO_2}-\varepsilon}{\varepsilon_{SiO_2}+2\varepsilon}+(1-f)\frac{\varepsilon_{VO_2}-\varepsilon}{\varepsilon_{VO_2}+2\varepsilon}=0. \quad (6)$$

Among which,

$$\varepsilon=\varepsilon_1+i\varepsilon_2 \quad (7)$$

$$\varepsilon_1=n^2-k^2 \quad (8)$$

$$\varepsilon_2=2nk \quad (9)$$

ε_{VO_2} and ε_{SiO_2} are the effective dielectric functions of the two nanoparticles, respectively. f denotes as the "filling factor" (*i.e.*, volume fraction) of SiO_2. ε_1 and ε_2 are the real part and the imaginary part of the dielectric function, respectively. The optical constants of VO_2 and SiO_2 are adopted from the literatures[19,51]. Based on the calculated optical constants of composite films with different f, we simulate the optical spectra of a single-layer composite film on borosilicate glass substrate by the Essential Macleod software.

1. Kamalisarvestani, M., Saidur, R., Mekhilef, S. & Javadi, F. S. Performance, materials and coating technologies of thermochromic thin films on smart windows. *Renew. Sust. Energ. Rev.* **26**, 353–364 (2013).
2. Ji, Y. D. *et al.* Role of microstructures on the M1-M2 phase transition in epitaxial VO_2 thin films. *Sci. Rep.* **4**, 4854 (2014).
3. Driscoll, T. *et al.* Memory Metamaterials. *Science* **325**, 1518–1521 (2009).
4. Qazilbash, M. M. *et al.* Mott transition in VO_2 revealed by infrared spectroscopy and nano-imaging. *Science* **318**, 1750–1753 (2007).
5. Li, S. Y., Niklasson, G. A. & Granqvist, C. G. Thermochromic fenestration with VO_2-based materials: Three challenges and how they can be met. *Thin Solid Films* **520**, 3823–3828 (2012).
6. Chae, B. G., Kim, H. T. & Yun, S. J. Characteristics of W- and Ti-doped VO_2 thin films prepared by sol-gel method. *Electrochem. Solid-State Lett.* **11**, D53–D55 (2008).
7. Patridge, C. J., Whittaker, L., Ravel, B. & Banerjee, S. Elucidating the influence of local structure perturbations on the metal-insulator transitions of $V_{1-x}Mo_xO_2$ nanowires: Mechanistic insights from an X-ray absorption spectroscopy study. *J. Phys. Chem. C* **116**, 3728–3736 (2012).
8. Batista, C., Carneiro, J., Ribeiro, R. M. & Teixeira, V. Reactive pulsed-DC sputtered Nb-doped VO_2 coatings for smart thermochromic windows. *J. Nanosci. Nanotechnol.* **11**, 9042–9045 (2011).
9. Manning, T. D., Parkin, I. P., Pemble, M. E., Sheel, D. & Vernardou, D. Intelligent window coatings: Atmospheric pressure chemical vapor deposition of tungsten-doped vanadium dioxide. *Chem. Mat.* **16**, 744–749 (2004).
10. Granqvist, C. G. Transparent conductors as solar energy materials: A panoramic review. *Sol. Energy Mater. Sol. Cells* **91**, 1529–1598 (2007).
11. Qazilbash, M. M. *et al.* Electrodynamics of the vanadium oxides VO_2 and V_2O_3. *Phys. Rev. B* **77**, 115121 (2008).

12. Verleur, H. W., Barker, A. S. & Berglund, C. N. Optical properties of VO_2 between 0.25 and 5 eV. *Phys. Rev. Lett.* **172**, 788 (1968).
13. Dai, L. *et al.* F-doped VO_2 nanoparticles for thermochromic energy-saving foils with modified color and enhanced solar-heat shielding ability. *Phys. Chem. Chem. Phys.* **15**, 11723–11729 (2013).
14. Zhou, J. D. *et al.* Mg-doped VO_2 nanoparticles: hydrothermal synthesis, enhanced visible transmittance and decreased metal-insulator transition temperature. *Phys. Chem. Chem. Phys.* **15**, 7505–7511 (2013).
15. Lee, M. H. & Cho, J. S. Better thermochromic glazing of windows with anti-reflection coating. *Thin Solid Films* **365**, 5–6 (2000).
16. Xu, G., Jin, P., Tazawa, M. & Yoshimura, K. Optimization of antireflection coating for VO_2-based energy efficient window. *Sol. Energy Mater. Sol. Cells* **83**, 29–37 (2004).
17. Kang, L. T. *et al.* Nanoporous thermochromic VO_2 films with low optical constants, enhanced luminous transmittance and thermochromic properties. *ACS Appl. Mater. Interfaces* **3**, 135–138 (2011).
18. Zhou, M. *et al.* Periodic porous thermochromic VO_2 (M) films with enhanced visible transmittance. *Chem. Commun.* **49**, 6021–6023 (2013).
19. Li, S. Y., Niklasson, G. A. & Granqvist, C. G. Nanothermochromics: Calculations for VO_2 nanoparticles in dielectric hosts show much improved luminous transmittance and solar energy transmittance modulation. *J. Appl. Phys.* **108**, 063525 (2010).
20. Li, Y. M., Ji, S. D., Gao, Y. F., Luo, H. J. & Kanehira, M. Core-shell VO_2@TiO_2 nanorods that combine thermochromic and photocatalytic properties for application as energy-saving smart coatings. *Sci. Rep.* **3**, 1370 (2013).
21. Gao, Y. F. *et al.* Enhanced chemical stability of VO_2 nanoparticles by the formation of SiO_2/VO_2 core/shell structures and the application to transparent and flexible VO_2-based composite foils with excellent thermochromic properties for solar heat control. *Energy Environ. Sci.* **5**, 6104–6110 (2012).
22. Li, R. *et al.* Synthesis and characterization of plate-like VO_2(M)@SiO_2 nanoparticles and their application to smart window. *Mater. Lett.* **110**, 241–244 (2013).
23. Chen, H. K., Hung, H. C., Yang, T. C. K. & Wang, S. F. The preparation and characterization of transparent nano-sized thermochromic VO_2-SiO_2 films from the sol-gel process. *J. Non-Cryst. Solids* **347**, 138–143 (2004).
24. Leroux, C., Nihoul, G. & Van Tendeloo, G. From VO_2 (B) to VO_2 (R): Theoretical structures of VO_2 polymorphs and in situ electron microscopy. *Phys. Rev. B* **57**, 5111–5121 (1998).
25. Zhao, L. L. *et al.* A low cost preparation of VO_2 thin films with improved thermochromic properties from a solution-based process. *Thin Solid Film* **543**, 157–161 (2013).
26. Lopez, R., Feldman, L. C. & Haglund, R. F. Size-dependent optical properties of VO_2 nanoparticle arrays. *Phys. Rev. Lett.* **93**, 177403 (2004).
27. Mlyuka, N. R., Niklasson, G. A. & Granqvist, C. G. Thermochromic multilayer films of VO_2 and TiO_2 with enhanced transmittance. *Sol. Energy Mater. Sol. Cells* **93**, 1685–1687 (2009).
28. Zhang, X. T. *et al.* Self-cleaning particle coating with antireflection properties. *Chem. Mater.* **17**, 696–700 (2005).
29. Born, M. & Wolf, E. *Principles of Optics*. 7th ed. (Cambridge University Press, Cambridge, UK, 1999).
30. Sun, Y. F. *et al.* New aspects of size-dependent metal-insulator transition in synthetic single-domain monoclinic vanadium dioxide nanocrystals. *Nanoscale* **3**, 4394–4401 (2011).
31. Kang, L. T. *et al.* Effects of annealing parameters on optical properties of thermochromic VO_2 films prepared in aqueous solution. *J. Phys. Chem. C* **114**, 1901–1911 (2010).
32. Jin, P., Xu, G., Tazawa, M. & Yoshimura, K. A VO_2-based multifunctional window with highly improved luminous transmittance. *Jpn. J. Appl. Phys., Part 2* **41**, L278–L280 (2002).
33. Mlyuka, N. R., Niklasson, G. A. & Granqvist, C. G. Thermochromic VO_2-based multilayer films with enhanced luminous transmittance and solar modulation. *Phys. Status Solidi A* **206**, 2155–2160 (2009).
34. Gao, Y. F. *et al.* VO_2-Sb: SnO_2 composite thermochromic smart glass foil. *Energ. Environ. Sci.* **5**, 8234–8237 (2012).
35. Liu, C., Wang, N. & Long, Y. Multifunctional overcoats on vanadium dioxide thermochromic thin films with enhanced luminous transmission and solar modulation, hydrophobicity and anti-oxidation. *Appl. Surf. Sci.* **283**, 222–226 (2013).
36. Lindstrom, R. *et al.* Thin films of vanadium oxide grown on vanadium metal: oxidation conditions to produce V_2O_5 films for Li-intercalation applications and characterisation by XPS, AFM, RBS/NRA. *Surf. Interface Anal.* **38**, 6–18 (2006).
37. Fu, G. H., Polity, A., Volbers, N. & Meyer, B. K. Annealing effects on VO_2 thin films deposited by reactive sputtering. *Thin Solid Films* **515**, 2519–2522 (2006).
38. Smith, G. B. & Granqvist, C. G. *Green Nanotechnology: Solutions for Sustainability and Energy in the Built Environment*. (CRC Press, Boca Raton, FL, 2010).
39. Kang, L. T. *et al.* Thermochromic properties and low emissivity of ZnO: Al/VO_2 double-layered films with a lowered phase transition temperature. *Sol. Energy Mater. Sol. Cells* **95**, 3189–3194 (2011).
40. Xu, G., Jin, P., Tazawa, M. & Yoshimura, K. Thickness dependence of optical properties of VO_2 thin films epitaxially grown on sapphire (0001). *Appl. Surf. Sci.* **244**, 449–452 (2005).
41. Kang, L. T. *et al.* Pt/VO_2 double-layered films combining thermochromic properties with low emissivity. *Sol. Energy Mater. Sol. Cells* **94**, 2078–2084 (2010).
42. Ramirez, J. G., Sharoni, A., Dubi, Y., Gomez, M. E. & Schuller, I. K. First-order reversal curve measurements of the metal-insulator transition in VO_2: Signatures of persistent metallic domains. *Phys. Rev. B* **79**, 235110 (2009).
43. Fan, W. *et al.* Large kinetic asymmetry in the metal-insulator transition nucleated at localized and extended defects. *Phys. Rev. B* **83**, 235102 (2011).
44. Lopez, R., Haynes, T. E., Boatner, L. A., Feldman, L. C. & Haglund, R. F. Size effects in the structural phase transition of VO_2 nanoparticles. *Phys. Rev. B* **65**, 224113 (2002).
45. Wu, C. *et al.* Direct hydrothermal synthesis of monoclinic VO_2 (M) single-domain nanorods on large scale displaying magnetocaloric effect. *J. Mater. Chem.* **21**, 4509–4517 (2011).
46. Tselev, A. *et al.* Interplay between Ferroelastic and Metal-Insulator Phase Transitions in Strained Quasi-Two-Dimensional VO_2 Nanoplatelets. *Nano Lett.* **10**, 2003–2011 (2010).
47. Niklasson, G. A., Granqvist, C. G. & Hunderi, O. Effective medium models for the optical-properties of inhomogeneous materials. *Appl. Opt.* **20**, 26–30 (1981).
48. Appavoo, K. *et al.* Role of Defects in the Phase Transition of VO_2 Nanoparticles Probed by Plasmon Resonance Spectroscopy. *Nano Lett.* **12**, 780–786 (2012).
49. Li, S. Y., Niklasson, G. A. & Granqvist, C. G. A thermochromic low-emittance coating: Calculations for nanocomposites of In_2O_3: Sn and VO_2. *Appl. Phys. Lett.* **99**, 131907 (2011).
50. Qazilbash, M. M. *et al.* Infrared spectroscopy and nano-imaging of the insulator-to-metal transition in vanadium dioxide. *Phys. Rev. B* **79**, 075107 (2009).
51. Gao, L., Lemarchand, F. & Lequime, M. Refractive index determination of SiO_2 layer in the UV/Vis/NIR range: Spectrophotometric reverse engineering on single and bi-layer designs. *J. Eur. Opt. Soc.-Rapid.* **8**, 13010 (2013).
52. Nag, J. & Haglund, R. F. Synthesis of vanadium dioxide thin films and nanoparticles. *J. Phys.: Condens. Matter* **20**, 264016 (2008).

Acknowledgments

This work was supported by National Natural Science Foundation of China (Grant No. 51172234), Guangdong Provincial Department of Industry and University Research (Grant No.2012B091000165) and the Opening Project of State Key Laboratory of High Performance Ceramics and Superfine Microstructure (Project No. SKL201204SIC).

Author contributions

M.L. proposed and organized the overall project. Z.L.L. performed the sample synthesis and optical analysis. L.C.Y. and S.H.R. carried out the theoretical calculation and ellipsometry measurement. L.C., T.A., K.Y.P. and G.H. accomplished TEM sample preparation and observation. All the authors discussed the results. Z.L.L. prepared the manuscript with discussion from M.L., T.S. and I.Y.

Additional information

Competing financial interests: The authors declare no competing financial interests.

How to cite this article: Zhao, L. *et al.* Solution-Processed VO_2-SiO_2 Composite Films with Simultaneously Enhanced Luminous Transmittance, Solar Modulation Ability and Anti-Oxidation property. *Sci. Rep.* **4**, 7000; DOI:10.1038/srep07000 (2014).